

Production of Biodiesel through Esterification of Palmitic Acid Using 12-Tungestophosphoric Acid Supported on Nanocavity of Aluminium Incorporated Mesoporous SBA-15¹

Razieh Fazaeli* and Hamid Aliyan

Department of Chemistry, Shahreza Branch, Islamic Azad University, 86145-311, Iran

*e-mail: fazaeli@iaush.ac.ir

Received May 5, 2015

Abstract—The main aim of this research is to develop efficient and environmentally benign heterogeneous catalysts for biodiesel production. For this purpose, H₃PW₁₂O₄₀ (PW₁₂) supported on Al-functionalized SBA-15 mesoporous molecular sieve featuring a well-defined three-dimensional (3D) mesoporosity were studied, and the prepared catalyst (PW₁₂/Al-SBA-15) was tested for the esterification process of palmitic acid to produce methyl palmitate as a kind of biodiesel. The effects of the methanol/oil ratio, catalyst amounts, reaction time, and reaction temperature on the conversion are also reported in this paper. More importantly, by using a 35 wt % of PW₁₂/Al-SBA-15 with methanol/oil molar ratio of 20 : 1 at reflux of methanol, the oil conversion of 98% after 8 h of reaction, could be achieved over the solid catalyst for at least 6 cycles under mild conditions.

DOI: 10.1134/S1070427215040217

INTRODUCTION

Biodiesel is an environmentally sustainable fuel composed of alkyl esters of long-chain fatty acids. It can be made from vegetable oils, animal fat, and waste oils from the food industry [1–5]. Currently, the most common process used for biodiesel production is through esterification of free fatty acids (FFAs) or catalytic transesterification of triglyceride with alcohols in the presence of a suitable catalyst [6–8].

Different heterogeneous base catalysts have been investigated for the production of biodiesel [9]. Some of these solid catalysts include alkali-metal and alkaline earth metal carbonates and oxides [5], lithium base ceramics [6], transition metal oxides [7], basic ion-exchange resins [8], layered double hydroxides [9] and zeolites [10].

In 1998, Zhao et al. synthesized a new type of mesoporous material SBA-15 with uniform two-dimensional hexagonal structure [11]. Compared with microporous zeolites, this material possesses significantly larger pores,

thicker pore walls, and higher hydrothermal stability. For these reasons, the discovery of SBA-15 provides a potential for the material as versatile catalysts and catalyst support for conversion of large molecules [12]. Since pure siliceous SBA-15 materials lack acidity, active centers must be introduced into their framework (mesoporous wall). Generally, incorporation of heteroatoms, such as Al into microporous zeolites will introduce a charge imbalance in the framework which is balanced by protons, thus generating bridging hydroxyl groups (SiOHAl, Bronsted acid sites) on these materials [13].

In continuation of our work on the catalytic properties of heteropoly acids (HPAs) [14,15], we focus our attention on the influence of PW₁₂/Al-SBA-15 as a catalyst in the esterification reaction of palmitic acid, where the parameters of temperature, time and reagent: catalyst molar ratios were examined.

EXPERIMENTAL

Synthesis of unmodified Al-SBA-15. Al-SBA-15 materials were prepared according to the direct synthesis procedure reported by Yue et al. [16] using aluminium

¹ The text was submitted by the authors in English.

isopropoxide as aluminium source and working with Si/Al molar ratios equal to 60.

Synthesis of 35% PW₁₂/Al-SBA-15. The supported PW₁₂ catalysts were prepared using the method of incipient wetness. In a typical process, a 560 mg portion of PW₁₂ was dissolved in deionized water and impregnated drop wise into 1960 mg support (Al-SBA-15) in 25 mL methanol, with constant agitation. The resulting pastes were dried for 4 h at 110°C and calcined for 4 h at 350°C.

Esterification procedures. The activity of the catalyst was examined through esterification of palmitic acid with methanol. All the esterification runs were carried out in a 250 mL round-bottom flask equipped with a reflux condenser and a magnetic stirrer. In a typical experiment, 0.15 g of palmitic acid was introduced into the flask, and then the temperature was increased to 95–100°C. After the palmitic acid had melted, 5 g of warm methanol and 0.2 g of 35 wt % PW₁₂/SBA-15 catalyst were quickly added and stirred rapidly by a magnetic bar at 600 rpm. (The weight ratio of palmitic acid to methanol was 1 : 20). The temperature of this liquid-phase esterification reaction was kept at 100°C for 8 h. Sample solutions were collected periodically from the flask during the reaction, and the concentration of the produced methyl palmitate was analyzed using a gas chromatograph. Ar was used as the carrier gas.

RESULTS AND DISCUSSION

Catalysts characterization. Figure 1a presents the FTIR spectra in the skeletal region of 4000–400 cm⁻¹ for the Al-SBA-15 and PW₁₂/Al-SBA-15 materials. For both of samples, a band at 3429 cm⁻¹ and 1636 cm⁻¹ assigned to the O–H stretching and bending vibration of physisorbed water [17]. Besides, the primary infrared bands related to the molecular sieves framework were the asymmetric and symmetric stretching of Si–O–Al at 1080 cm⁻¹ and 803 cm⁻¹, and the absorption peak at 463 cm⁻¹ could be ascribed to the Si–O–Al bending stretching vibration [18]. Both of spectra of Al-SBA-15 and PW₁₂/Al-SBA-15 exhibit intensive absorption bands at 1080 and 803 cm⁻¹, which arise from the silica host matrix [19]. The FT-IR spectra of the PW₁₂/Al-SBA-15 indicate that most of the characteristic bands of the parent Keggin structure, which could be found in the PW₁₂ fingerprint region (1250–500 cm⁻¹), are not shown or appeared in the same assignable position of the bands corresponding to the ordered mesoporous silica host materials.

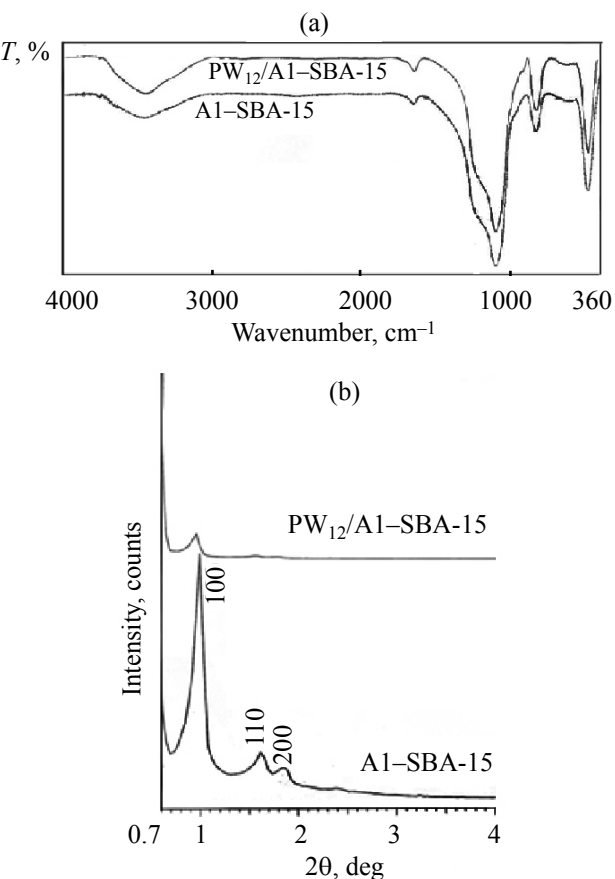


Fig. 1. (a) FTIR spectrum, (b) XRD patterns of Al-SBA-15 and PW₁₂/Al-SBA-15.

Figure 1b shows XRD patterns of parent Al-SBA-15 within the 2θ range of 0.7–5. Small-angle X-ray diffraction patterns of parent Al-SBA-15 materials represent intensive well-resolved peaks, which can be indexed as the (100), (110), and (200) reflections of a 2-D hexagonal lattice with *p*6mm symmetry [20]. PW₁₂ introduction leads to a significant decrease in the intensity of the reflections. All patterns in the figures show a main diffraction peak due to *d*(100) reflection of SBA-15 hexagonal space group *p*6mm. At higher 2θ angles, *d*(110) and *d*(200) reflections are not observed, indicating that the adopted synthesis procedure leads to less ordered materials than traditional Al-SBA-15 [21].

TEM images of selected PW₁₂/Al-SBA-15 are presented in Fig. 2. A well-resolved contrast characteristic of certain silica mesopore structure symmetry is still observed, which is an indication for the preservation of the long ordered arrangement of the channels in the silica

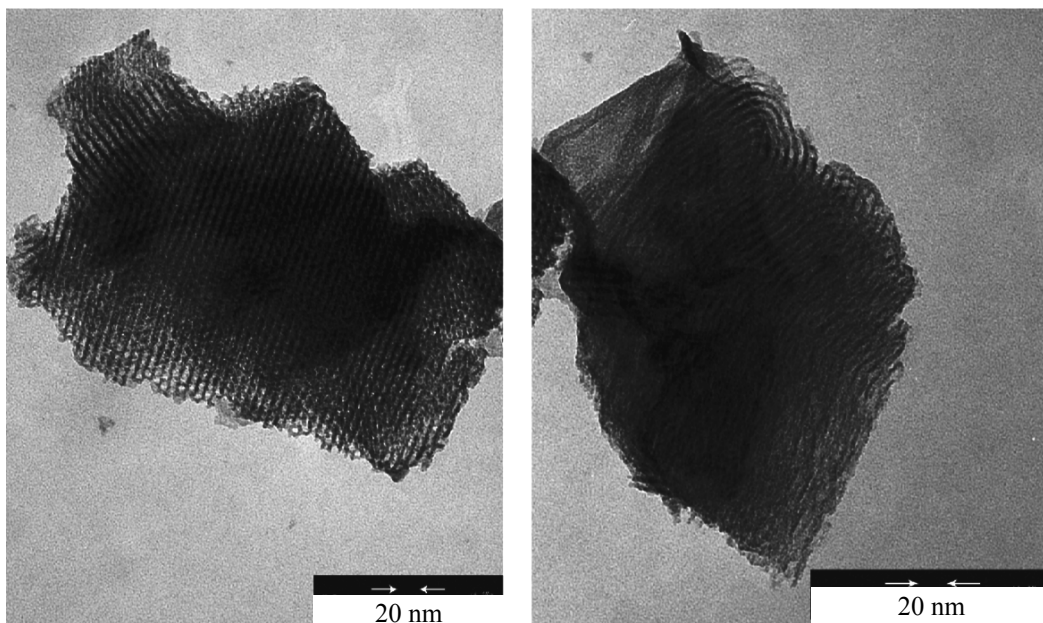


Fig. 2. TEM images of PW₁₂/Al-SBA-15.

host matrix after the aluminium deposition. The places with darker contrast could be assigned to the presence of PW₁₂ particles with different dispersion. The small dark spots in the images could be ascribed to PW₁₂ particles, probably located into the support channels. The larger dark areas over the channels most likely correspond to PW₁₂ agglomerates on the external surface.

The content of PW₁₂ on the Al-SBA-15 supports, which was calculated from W content in supported Al-SBA-15 was determined by neutron activation analysis (NAA). The good distribution of elements analyzed is in agreement with the neutron activation analysis (NAA) and ICP results with deviation in the range of ±0.09.

N₂ adsorption–desorption isotherms. Figure 3 shows the N₂ adsorption–desorption isotherms and pore size distributions of Al-SBA-15 and PW₁₂/Al-SBA-15. All the samples exhibited typical IV type isotherms and H1 type hysteresis loops at high relative pressures according to the IUPAC nomenclature [22], which are the typical characteristics of mesoporous materials [23]. The

PW₁₂/Al-SBA-15 showed very similar isotherm pattern and pore size distribution compared to bare Al-SBA-15, indicating that the mesopore structure of mesoporous silica was still maintained even after the surface modification step and the subsequent immobilization step of PW₁₂. Physical properties of parent Al-SBA-15, PW₁₂ (bulk) and modified Al-SBA-15 are listed in Table 1. As expected, the BET surface areas and total pore volumes of bare Al-SBA-15 are decreased after the functionalization with PW₁₂. These changes reflect that part of the mesopore volume in the Al-SBA-15 matrix is filled with PW₁₂.

Catalytic performance. Effect of molar ratio of alcohol to acid on the esterification reaction. The esterification is a reversible reaction so that excessive alcohol was usually added in order to improve the conversion. In the present work, the effect of different molar ratios of palmitic acid to methanol (12 : 1–24 : 1) was studied (Fig. 4a). The decrease of conversion was observed when the molar ratio exceeded 20 : 1. It

The texture parameters of bare Al-SBA-15 and PW₁₂/Al-SBA-15 in comparison with the bulk PW₁₂ materials

Entry	Sample	BET, surface area, m ² g ⁻¹	Pore volume, cm ³ g ⁻¹	Pore diameter, nm
1	Al-SBA-15	1041	1.2	4.6
2	PW ₁₂	6	—	—
3	PW ₁₂ /Al-SBA-15	75	0.71	3.61

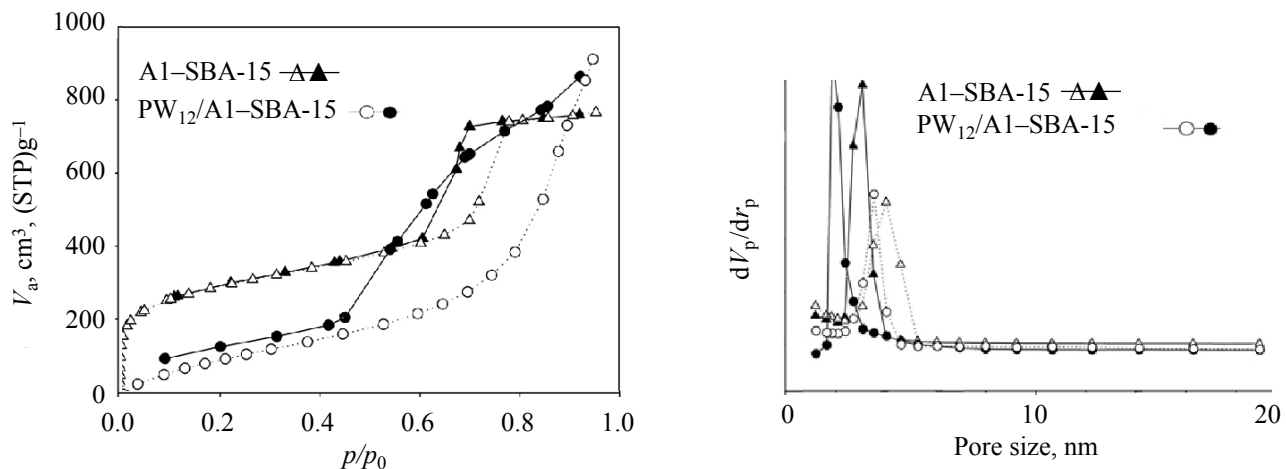


Fig. 3. (a) N_2 -Adsorption-desorption isotherms and (b) pore size distributions calculated by the BJH method of Al-SBA-15 and PW₁₂/Al-SBA-15.

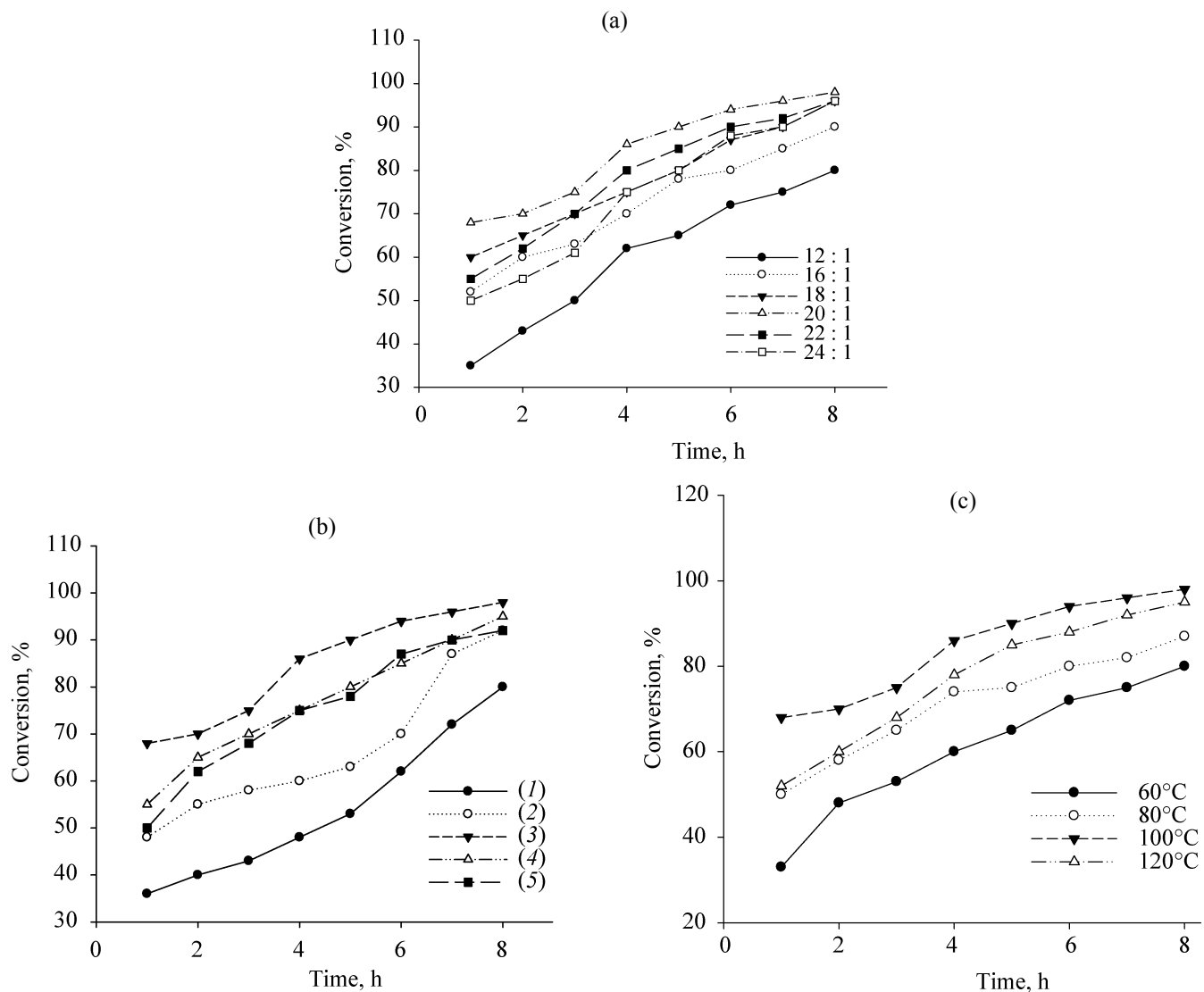


Fig. 4. Effect of (a) molar ratio of methanol to oil on the esterification reaction; (b) catalyst loading on the esterification reaction and (c) temperature on the esterification reaction.

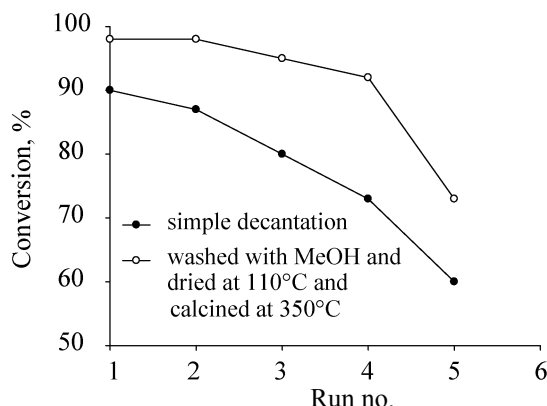


Fig. 5. Reusability study after five reaction cycles for 35 wt % $\text{PW}_{12}/\text{Al-SBA-15}$ catalyst, reaction conditions: catalyst amount 2 g, methanol/oil molar ratio 20 : 1, reaction time 8 h, reaction temperature 100°C.

continues to decrease upon the ratio is further increased to 24 : 1. It is speculated that the further excess methanol molecules may flood the active sites of the catalyst which hinder the protonation of palmitic acid at the active sites [3, 24].

Effect of catalyst dosage. Another important parameter that affects the ester yield is the catalyst dosage. In a screening experiment, different PW_{12} loading (final PW_{12} content of 25–45 wt %) were used for the catalyst preparation, and the esterification reaction was carried out over the as-prepared solid catalysts. Based on the experimental results, the 35% $\text{PW}_{12}/\text{Al-SBA-15}$ (Fig. 4b) was found to be the most active catalyst for the esterification reaction. The increase in the reaction rate (from 25 to 35 wt %) was due to the increase in the total number of active sites available for the reaction with increasing catalyst loading [25]. The decrease in the reaction rate (from 35 to 45 wt %) was perhaps attributed to the blocking of the active sites due to formation of multilayer on the support, and the multilayer formation can hinder the reactant molecules to react with the active sites. Thus, there is decrease in the conversion [26].

Effect of reaction temperature. The effect of reaction temperature on the esterification of palmitic acid was studied in the range of 60–120°C. For the esterification of palmitic acid with methanol (1 : 20) using 35 wt % $\text{PW}_{12}/\text{Al-SBA-15}$ four different temperatures (60, 80, 100, and 120°C) were used (Fig. 4c). The results show that the biodiesel yield increases with an increasing the reaction temperature and the maximum biodiesel yield of 98% is obtained at 100°C. Since the esterification

reaction is endothermic in nature, it favors a higher reaction temperature for biodiesel synthesis [27]. When the reaction temperature is increased to above 100°C, the biodiesel yield (%) decreases. There was a chance of loss of alcohol and increasing of darkness color of the product at higher temperature [28].

Recycling of the catalyst. The catalyst reusability is an important feature for determining its commercial viability. The catalyst was recycled to test its activity as well as stability. The catalyst was separated from the reaction mixture by filtration, washed with methanol until the filtrate is free from the acid, e.g., unreacted palmitic acid if any, followed by washing with double distilled water and then dried at 110°C and calcined at 350°C. No appreciable change in activity was noticed after four cycles (Fig. 5).

CONCLUSIONS

The performance of $\text{H}_3\text{PW}_{12}\text{O}_{40}$ -supported on aluminum-mesoporous silica (Al-SBA-15) as catalyst prepared by impregnation method in esterification of palmitic acid is outstanding. It demonstrates high catalytic activity and long durability in esterification of palmitic acid, in which the fatty acid methyl ester yield reached 98% consecutively for 4 cycles even under mild conditions (methanol/palmitic acid = 20 : 1, 35 wt % of catalyst, 100°C, 8 h). From the results of this study, it is proposed that $\text{PW}_{12}/\text{Al-SBA-15}$ is a suitable catalyst for the production of methyl palmitate by the esterification of palmitic acid owing to the high acid site density.

ACKNOWLEDGMENTS

We gratefully thank Shahreza Branch, Islamic Azad University, for financial support.

REFERENCES

1. Borugadda, V.B. and Goud, V.V., *Renew. Sustain. Energy Rev.*, 2012, vol. 16, pp. 4763–4784.
2. Chouhan, A.P.S. and Sarma, A.K., *Renew. Sustain. Energy Rev.*, 2011, vol. 15, pp. 4378–4399.
3. Zhang, Yue, Wong, Wing-Tak, and Yung, Ka-Fu, *Applied Energy*, 2014, vol. 116, pp. 191–198.
4. Luque, R., Lovett, J.C., Datta, B., Clancy, J., Campelo, J.M., and Romero, A.A., *Energy & Env. Sci.*, 2010, vol. 3, pp. 1706–1721.
5. Liu, X., He, H., Wang, Y., Zhu, S., and Piao, X., *Fuel*, 2008,

- vol. 87, pp. 216–221.
6. Wang, J.X., Chen, K.T., Huang, J.S.S.T., and Chen, C.C., *Chin. Chem. Lett.*, 2011, vol. 22, pp. 1363–1366.
 7. Singh, A.K. and Fernando, S.D., *Energy & Fuels*, 2008, vol. 22, pp. 2067–2069.
 8. Shibasaki-Kitakawa, N., Honda, H., Kurabayashi, H., Toda, T., Fukumura, T., and Yonemoto, T., *Bioresource Technology*, 2007, vol. 98, pp. 416–421.
 9. Shumaker, J.L., Crofcheck, C., Tackett, S.A., Santillan-Jimenez, E., Morgan, T., Ji, Y., Crocker, M., and Toops, T.J., *Appl. Catal. B: Env.*, 2008, vol. 82, pp. 120–130.
 10. Suppes, G.J., Bockwinkel, K., Lucas, S., Botts, J.B., Mason, M.H., and Heppert, J.A., *J. Am. Oil Chemists Soc.*, 2001, vol. 78, pp. 139–145.
 11. Zhao, D., Feng, J., Huo, Q., Melosh, N., Fredrickson, G.H., Chmelka, B.F., and Stucky, G.D., *Science*, 1998, vol. 279, p. 548.
 12. Taguchi, A. and Schuth, F., *Microporous Mesoporous Mater.*, 2005, vol. 77, pp. 1–45.
 13. Hu, W., Luo, Q., Su, Y., Chen, L., Yue, Y., Ye, C., and Deng, F., *Microporous and Mesoporous Materials*, 2006, vol. 92, pp. 22–30.
 14. Fazaeli, R. and Aliyan, H., *Appl. Catal. A: Gen.*, 2007, vol. 331, pp. 78–83.
 15. Fazaeli, R. and Aliyan, H., *Appl. Catal. A: Gen.*, 2009, vol. 353, pp. 74–79.
 16. Yue, Y., Gédéon, A., Bonardet, J.-L., Melosh, N., and D’Espinose, J.-B., *J. Fraissard, Chem. Commun.*, 1999, vol. 19, pp. 1967–1968.
 17. Nakamoto, K., *Infrared Spectra of Inorganic and Coordination Compounds*, New York: Wiley, 2009.
 18. Lombardo, M.V., Videla, M., Calvo, A., Requejo, F.G., and Soler-Illia, G.J.A.A., *J. Hazard. Mater.*, 2012, vols. 223–224, pp. 53–62.
 19. Feng, X., Fryxell, G.E., Wang, L.Q., Kim, A.Y., Liu, J., and Kemner, K.M., *Science*, 1997, vol. 276, pp. 923–926.
 20. Choi, M., Heo, W., Kleitz, F., and Ryoo, R., *Chem. Commun.*, 2003, pp. 2136–2137.
 21. Tsioncheva, T., Ivanova, L., Rosenholm, J., and Linden, M., *Appl. Catal. B: Env.*, 2009, vol. 89, pp. 365–374.
 22. Sing, K.S.W., Everett, D.H., Haul, R.A.W., Moscou, L., and Pierotti, R.A., *J. Rouquerol, Pure Appl. Chem.*, 1985, vol. 57, pp. 603–619.
 23. Beck, J.S., Vartuli, J.C., Roth, W.J., Leonowicz, M.E., Kresge, C.T., and Schmitt, K.D., *J. Am. Chem. Soc.*, 1992, vol. 114, pp. 10834–10843.
 24. Juan, J.C., Zhang, J., Jiang, Y., Cao, W., and Yarmo, M.A., *Catal. Lett.*, 2007, vol. 117, pp. 153–158.
 25. Jiang, Y., Lu, J., Sun, K., Ma, L., and Ding, J., *Energy Convers Manage*, 2013, vol. 76, pp. 980–985.
 26. Patel, A. and Singh, S., *Fuel*, 2014, vol. 118, pp. 358–364.
 27. Yu, X., Wen, Z., Li, H., and Tu, S-T., *J. Yan. Fuel*, 2011, vol. 90, pp. 1868–1874.
 28. Chongkhong, S., Tongurai, C., Chetpattananondh, P., and Bunyakan, C., *Biomass Bioenergy*, 2007, vol. 31, pp. 563–568.